Proceedings of the 21st ICSMGE, Vienna, Austria, 14 – 19 June 2026. Pistrol, Adam & Schweiger (eds.)
Published by: ÖGG, Austrian Society for Geomechanics, Salzburg, Austria, ISBN 978-3-9503898-4-5
https://doi.org/10.53243/ICSMGE2026-107

A special case of geotechnical characterization for an electrical substation located in the Mexico Valley

Rafael Ortiz Hernández, Raúl Bernal Luna, Óscar Jesús Luna González
Gerencia de Estudios de Ingeniería Civil, Comisión Federal de Electricidad, México, rafael.ortizh@cfe.mx

ABSTRACT: This study presents the geotechnical studies performed for the foundation and earth retention system design for an electrical substation to be constructed in the Mexico Valley with a special case of geotechnical properties such as uneven layered soft soils with high Overconsolidation Ratios, embedded dense sand/volcanic ash lenses, deep soft soil deposits, a high site dominant vibration period and great seismic amplification. For site characterization Piezocone (CPTu), Standard Penetration Testing (SPT), selective undisturbed soil sampling (SS), Field Vane Shear Test (VST), Phicometer (PhMT), and Menard Pressuremeter (PMT) was performed. Complementarily geophysical surveys (seismic cross-hole, and dynamic characterization using microtremor on the ground surface), also piezometric transducers and topographical references were installed at different depths for monitoring during the lifetime of the substation was carried out. Geotechnical laboratory testing with the goal of having high-quality data to determine the properties of the subsoil to use in constitutive models such as Soft Soil and Hardening Soil was accomplished. The derived ground model for undrained and drained conditions, standard and intermediate constitutive modelling yielded a deep foundation solution for the main structures and a braced diaphragm wall. Both solutions have a satisfactory Ultimate Limit and Service State for the short and long-term performance of this project, according to the Mexico foundation design regulations.

KEYWORDS: Soft soils; in-situ testing; laboratory testing; advanced soils models.

1 INTRODUCTION

In the framework of the continuous improvement of the electrical grid in the Metropolitan Area of the Valley of Mexico (MAVM), pre-existing substations are being considered for expansion. The Federal Electricity Commission (CFE), the state entity in charge of designing, operating, and maintaining Mexico's electrical infrastructure is tasked with such endeavor. Within the organizational structure of the CFE, the Civil Engineering Studies Management (GEIC-CFE) has played a crucial role in the development of such projects.

The GEIC-CFE houses the Department of Soil Mechanics, whose mission is to provide the best geotechnical engineering service for the development of national infrastructure projects. With the significant advantage of having direct exploration equipment and a wide range of in-situ tests, in addition to a highly equipped soil mechanics laboratory, it has the availability of the necessary inputs for the proper geotechnical site characterization for any project. This advantage allows for an ample quantity and quality of information, enabling the geotechnical engineer to make informed decisions based on technical and scientific aspects.

2 SITE LOCATION AND PREVIOUS RESEARCH

The site of the substation is located on the border between the State of Mexico and Mexico City, in the southeastern area of the MAVM. According to the regional geotechnical zoning of Mexico City (GCDMX, 2023a), the site is situated in what is referred to as Zone III. Lacustrine (Figure 1). This zone comprises thick deposits of highly compressible clay, separated by layers of sandy soil, ranging from moderately compact to very compact, with varying contents of volcanic ash, silt, or clay, and with thickness varying from centimeters to several meters.

The site is in an area that experiences a regional subsidence rate ranging between 0.30 and 0.35 m/year (GCDMX, 2023a citing Juárez et al, 2022) as shown in Figure 2. This subsidence is a consequence of the consolidation of deep deposits due to the extraction of groundwater for domestic use.

The project involved the construction of two main buildings: the first building (Building A) consists of 6 levels with a footprint of 16.35 m wide by 24.35 m long; and the second building (Building B) consists of 1 level with a footprint of 8.20 m wide by 22.28 m long. Both structures require a foundation box of 5.20 m for underground facility connections as seen in Figure 3.

3 GEOTECHNICAL SITE EXPLORATION

The original exploration campaign included the execution of 3 test pit excavations (PCA) with volumetric pits (CV), 1 standard penetration test (SPT) to a depth of 50 m, 1 selective survey (SS) with undisturbed sampling and field vane tests (VST) down to a 45 m depth; in addition to 2 piezocone soundings (CPTu) down to a 50 m depth. Furthermore, 3 points of seismic microzoning (MS) and 1 cross-hole test (CH) down to a 45 m depth were conducted.

As a complementary measure, a 1 semi-deep level benchmark at a depth of 50 m was installed along with 1 observation well at 7 m depth and 1 piezometric station consisting of 4 push-in type vibrating wire piezometers.

The test pit excavations were used to determine the surface stratigraphy. The maximum depth reached in the pits was 2.20 m, and a very shallow groundwater level was encountered at 0.60 m depth. Upon detecting a layer of superficial fill composed of coarse granular material (sand and gravel), unit weights testing was performed to determine its bulk density.

For the exploration of deep stratigraphy, an initial continuous standard penetration test (SPT-1) was conducted until a depth of 70 m was reached, as the layer commonly known as the 'First Hard Layer' was not encountered within the initial 50 m explored. With the resistance profile of the number of SPT blows, the recovered materials, and their respective water content, an initial stratigraphic model was constructed, which was subsequently used for the interpretation of CPTu tests and the feasibility of conducting borehole tests.

A piezocone test (CPTu-1) was conducted approximately 25 m north of the SPT borehole expecting a similar stratigraphy. However, the resistance profile and normalized Soil Behavior Type (SBT_n) indicated a significant difference in the thickness of the stratigraphy identified in the SPT. Three additional CPTu tests were conducted, in addition to those already scheduled, resulting in a total of 5 tests, located at various points on the site, anticipating a high variability in the subsurface conditions. The maximum exploration depth of CPTu soundings was 59.70 m. In the draining lenses (identified as sands based on their SBT_n), pore pressure dissipation tests were conducted to determine the pore pressure profile of the site, with a duration of 1,000 s or until the pressure stabilized significantly.

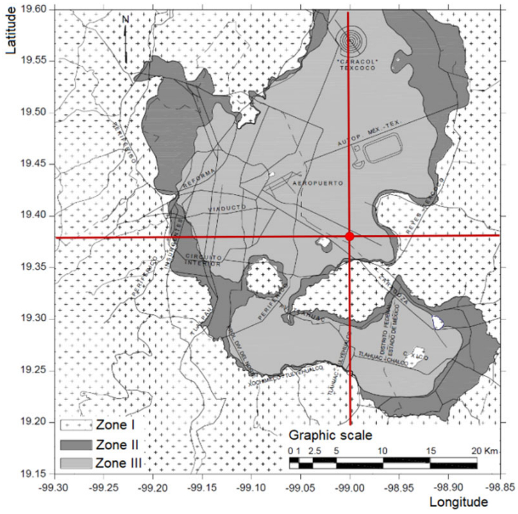

Figure 1. Location of the study site in the geotechnical zoning of the Valley of Mexico (Modified from NTC-DCC-CDMX, 2023).

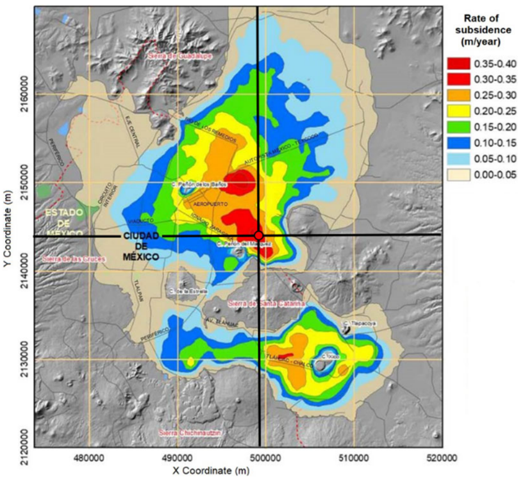

Figure 2. Location of study site with respect to the regional subsidence of the Valley of Mexico (Modified from GCDMX, 2023a).

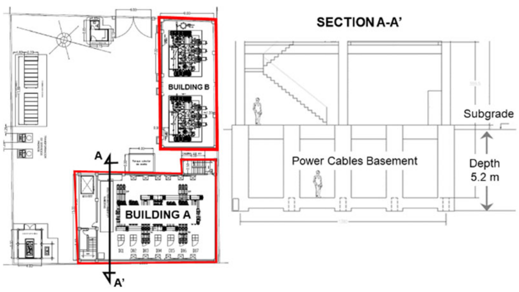

Figure 3. Building location plan and section showing the basement of Building B.

To obtain laboratory data on shear strength, deformation, and compressibility properties, two selective surveys (SS) were conducted in the vicinity of CPTu-1. In SS-1, sampling was performed using a 0.10 diameter thin-walled tube sampler, to a maximum depth of 35 m. In the second survey (SS-2), 3 shear strength tests (peak and residual) were conducted using a field vane (VST) at depths of 6, 16, and 33 m, along with undisturbed sampling of fine materials at greater depths (approximately 50 m).

Due to the presence of granular materials (sands) that were not initially anticipated in the original scope, it was necessary to conduct an in-situ testing (SPI) survey using a phicometer (PhMT) at 17.50 m depth and a Menard pressuremeter (PMT) at 16.50 m depth to determine strength and deformation parameters. Additionally, additional field vane tests (VST) were conducted for fine soils at depths of interest (9.6 and 30 m).

As part of the dynamic characterization, a seismic Cross-Hole test (at a depth of 44 m) and three measurements of ambient noise (MS) were conducted.

Finally, to monitor the long-term behavior of the structures and during the construction stage, an altimetric and piezometric monitoring station was installed. This station included two floating level benchmarks (at depths of 20 and 59 m), a water observation well (at a depth of 5.9 m), three push-in type vibrating wire piezometers (at approximate depths of 12, 32, and 43 m respectively), and a vibrating wire piezometer within a Casagrande-type piezometric chamber (at a depth of 23 m).

The layout of the surveys, field tests, and monitoring instruments proposed across two parcels, which were ultimately unified, is shown in Figure 4. Meanwhile, Figure 5 provides a three-dimensional schematic illustrating the locations and depths of the boreholes, tests, and instruments installed on-site.

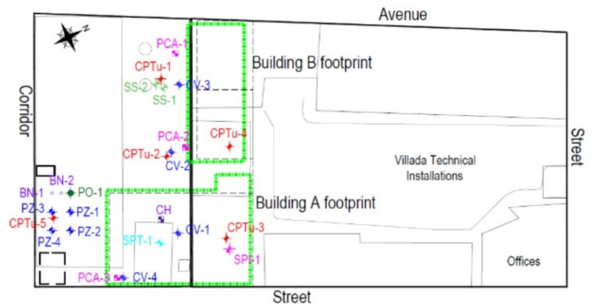

Figure 4. Location of surveys, field tests and on-site instrumentation.

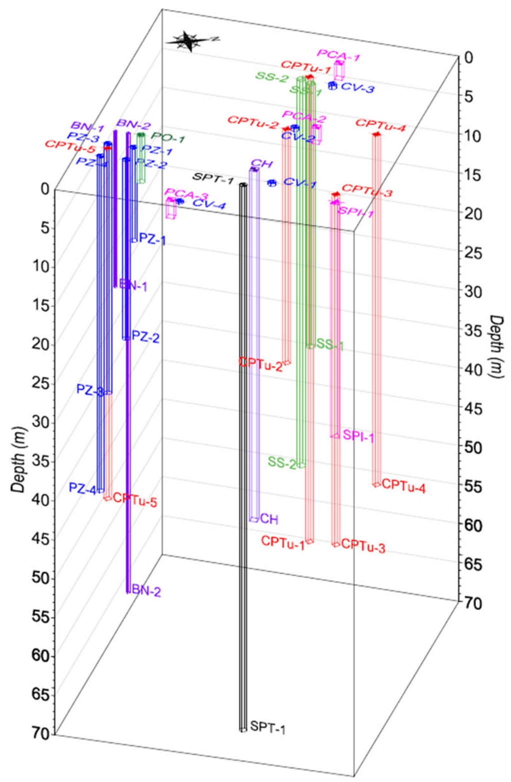

Figure 5. Depths reached in boreholes, field tests and on-site instrumentation.

4 LABORATORY TESTING

In the samples recovered from the SPT and SS boreholes, visual and manual classification tests, water content analysis, Atterberg limits determination, particle size distribution analysis, determination of fines content, and density of the soil solids measurements were conducted.

In the undisturbed samples, determinations of shear strength were conducted using non-consolidated undrained (Tx-UU), consolidated undrained (Tx-CU), and loading-reloading (Tx-CU_{ur}) triaxial compression tests. Regarding the acquisition of compressibility parameters, conventional one-dimensional consolidation tests and tests with a cycle of loading, unloading, and reloading were performed.

No dynamic geotechnical testing was performed as geotechnical earthquake engineering was beyond the scope of this design.

The results of the tests were used as input for the calibration of intermediate soil constitutive models, which will be discussed later.

5 RESULTS

5.1 *Stratigraphy*

The samples from SPT-1 were used to determine the materials composing the stratigraphic units of the site subsurface, including a superficial fill, and correlated with the behaviors of materials found in the piezocones. The description by stratigraphic unit was conducted according to the Unified Soil Classification System (USCS) and is presented below:

1. Gray and greenish-grey clay with high plasticity and soft consistency.
2. Greenish brown and reddish-brown clay with high plasticity and a very soft consistency.
3. Reddish-brown clay with high plasticity and very soft consistency.
4. Intercalations of gravely sand with loose to very loose compactness and sandy clay of the same color with very soft consistency.
5. Greenish-brown clay and clay with fine sand of the same color with high plasticity and very soft consistency.
6. Fine sand and dark brown clayey fine sand with dense to very dense compactness.
7. Clayey sand with medium consistency.
8. Intercalations of greenish-brown clay and sandy clay with high plasticity and very soft consistency with fine sand with dark brown clay with very loose compactness.
9. Fine sand with dark brown clay of loose to medium compactness.
10. Clay and sandy clay with various shades of brown with high plasticity and very soft consistency.

The stratigraphic unit 6 was not detected in the SPT-1 borehole, so the description of the material comes from the SBT_n index of the piezocones that did detect this layer. Additionally, it is worth mentioning that a tezontle fill was superficially identified, which is volcanic sand with gravel.

A three-dimensional model of the stratigraphy of the site, generated using PLAXIS 3D v20.0 software is shown in Figure 6.

5.2 *Hydraulic conditions*

The pore pressure dissipation tests indicate that the site is under hydrostatic conditions down to the maximum testing depth of 59.7 m ((Figure 7). This is consistent with the measurements obtained from the piezometers at the monitoring station, after the instrument stabilization period due to installation effects.

This hydrostatic condition differs from conventional measurements in the Mexico Valley as it doesn't have a reduction on pore pressure due to underground pumping (Auvinet et al, 2017).

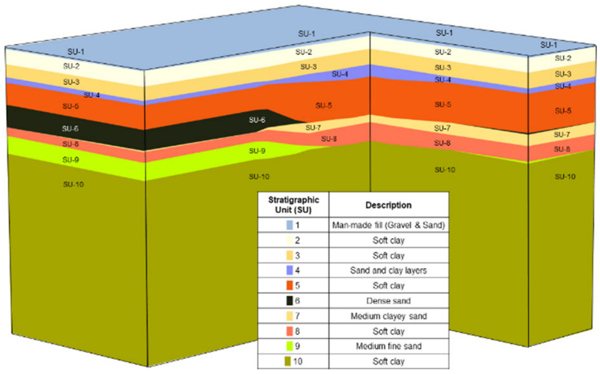

Figure 6. Three-dimensional stratigraphic model of the site

5.3 *Geotechnical Models*

The surface exploration (PCA) allowed us to identify materials associated with anthropic fills and natural materials, where for both cases, thicknesses and bulk densities were identified.

From the execution of the SPT borehole, it was possible to obtain representative samples for water content determinations, which in turn made it possible to verify the behavior of some parameters (C_c, C_r, e_0) with correlations in the existing literature and from a proprietary database of GEIC-CFE. Preliminary strength and deformation parameters were calculated with established correlations with the N_{60} (Briaud, 2023), considering a measured efficiency of 74% from a SPT Analyzer measurement.

In the case of CPTu, in addition to the parameters directly obtained from the test, such as cone tip resistance (q_t), sleeve friction (f_s), and pore pressure during penetration (u_d), correlations collected by Robertson and Cabal (2022) were used to obtain undrained shear strength (s_u), undrained elastic modulus (E_u), preconsolidation ratio (OCR), effective friction angle for coarse grained soils (φ') and permeability (k).

The N_{kt} value for s_u was determined based on the peak undrained shear strength value from VST, with an N_{kt} value ranging between 8 and 13. The correlation for E_u, Equation (1), is a proposal from GEIC-CFE based on laboratory test results of materials from the Valley of Mexico.

$$E_u(MPa) = 0.128s_u + 0.454 \quad (1)$$

Upon analyzing the results of consolidation laboratory tests, it was observed that the correlations for the preconsolidation ratio from the CPTu did not yield consistent results, thus these correlations were discarded

The CPTu correlation for internal friction angle for granular soils was also discarded for determining lower values than those recorded in literature (Auvinet et al, 2017).

In the case of the VST, PhMT, and PMT, they served as reference points for the geotechnical engineer in the interpretation of information for the final assignment of strength and deformation parameters of the geotechnical model.

Due to the project requirements, it was necessary to generate multiple geotechnical models to address the ultimate limit state (ULS) (Total Stress Mohr-Coulomb models, Tables 1 and 2) and serviceability limit state (SLS) designs of the foundation of the structures and excavation support system. The serviceability limit state analysis of both had to be performed through computational numerical analysis (Effective Stress Mohr-Coulomb, Hardening Soil and Soft Soil models, Tables 3 to 6).

Due to the significant variation in the stratigraphic configuration of the site, it was decided to zone the site for the two main structures as described in Section 2.

5.4 *Total Stress Mohr Coulomb Model*

In this model (Tables 1 and 2) the undrained shear strength (s_u) parameters for each unit were defined based on the interpretation of the CPTu, VST and Tx-UU tests. The undrained elastic moduli (E_u) were determined by a correlation with the CPTu shear strength validated with results from Tx-UU tests. The undrained Poisson's ratio (ν_u) was assigned according to the type of material and published literature (Auvinet, 2019 and Ibarra et al, 2018).

Table 1. Building A Total Stress Mohr-Coulomb Model.

GU	Depth	γ_{nat} (kN/m³)	s_u (kPa)	E_u (kPa)	ν_u
1	0.00 – 0.35	15.35	80	6,000	0.35
2	0.35 – 4.05	13.82	30	3,441	0.45
5	4.05 – 8.55	11.51	20	2,225	0.45
6	8.55 – 13.80	11.60	28	2,463	0.45
7	13.80 – 19.35	20.10	160	10,917	0.38
8	19.35 – 21.45	13.00	95	9,811	0.45
9	21.45 – 25.80	16.50	200	6,400	0.38
10	25.80 – 70.00	11.20	78	8,145	0.45

Table 2. Building B Total Stress Mohr-Coulomb Model.

GU	Depth	γ_{nat} (kN/m³)	s_u (kPa)	E_u (kPa)	ν_u
2	0.00 – 3.16	13.82	27	3,147	0.45
3	3.16 – 6.98	11.51	20	2,225	0.45
4	6.98 – 8.38	11.51	20	2,225	0.35
5	8.38 – 18.06	11.60	29	2,463	0.45
7	18.06 – 21.04	14.00	150	4,250	0.40
8	21.04 – 23.29	13.00	40	4,421	0.45
10	23.29 – 70.00	11.20	40	4,421	0.45

5.5 *Effective Stress Mohr Coulomb Model*

Effective strength values (apparent cohesion, $c'$and internal friction angle, ϕ') in fine materials were obtained from triaxial laboratory tests of unaltered samples in undrained consolidated condition. In granular materials (such as units 4, 6, 7 and 9), a correlation with CPTu was used for internal friction angles and an apparent cohesion value of 1 kPa was assigned for numerical stability purposes. Regarding the drained elastic modulus (E') values, the determination was made using the expression in Equation 2 (Budhu, 2011):

$$E' = \frac{E_u}{1 - \nu'} \qquad (2)$$

Regarding coarse materials, a correlation with the number of N_{60} blows was used. The value of the effective Poisson's ratio (ν') was considered as a constant of 0.33 for all materials.

The permeability of coarse-grained soils was determined with CPTu correlations and for fine grained soils, it was determined with consolidation testing values.

Table 3 and 4 present the effective stress Mohr-Coulomb geotechnical values for Building A and B, respectively.

Table 3. Building A Effective Stress Mohr-Coulomb Model.

GU	c' (kPa)	ϕ' (°)	E' (kPa)	ν'	k (m/s)
1	1	28	6,300	0.33	4.0×10^{0}
2	6	33	3,051	0.33	2.3×10^{-3}
5	0	34	1,973	0.33	2.9×10^{-5}
6	8	33	2,184	0.33	2.2×10^{-9}
7	1	39	23,990	0.33	5.9×10^{-9}
8	1	32	8,699	0.33	3.1×10^{-9}
9	1	30	14,639	0.33	7.2×10^{-2}
10	37	21	7,222	0.33	3.5×10^{-9}

Table 4. Building A Effective Stress Mohr-Coulomb Model.

GU	c' (kPa)	ϕ' (°)	E' (kPa)	ν'	k (m/s)
2	6	33	2790	0.33	2.3×10^{-3}
3	1	34	1973	0.33	2.9×10^{-5}
4	1	30	12403	0.33	8.6×10^{0}
5	8	33	2184	0.33	3.6×10^{-4}
7	1	30	13814	0.33	5.9×10^{-9}
8	1	32	3920	0.33	3.1×10^{-9}
10	37	21	3920	0.33	3.5×10^{-9}

5.6 *Hardening Soil Model*

This model, show in Table 5, was determined for fine-grained soil layers. The strength parameters were declared as in the effective stress Mohr-Coulomb model. The reference deformation modulus at 50% (E_{50}^{ref}) was obtained from the stress-strain curves of the undrained consolidated triaxial compression tests. The oedometric modulus (E_{oed}) was determined from the stress-strain curves of the consolidation tests. The power value of stress dependence (m) was assigned as 1.0 according to experience with this type of materials. The unloading-reloading Poisson's ratio (ν_{ur}) is maintained as a constant of 0.20 for all materials (Bentley, 2023). For granular materials in the numerical models, only the effective stress parameters were declared (Tables 3 and 4).

Table 5. Building A & B Hardening Soil Model.

GU	E_{50}^{ref} (kPa)	E_{ur}^{ref} (kPa)	E_{oed}^{ref} (kPa)	m	ν_{ur}
2	15,067	15,067	45,201	1	0.20
5	3,215	280	9,646	1	0.20
8	2,809	454	6,980	1	0.20
10	7,304	4,209	10,103	1	0.20

5.7 *Soft Soil Model*

Like the Hardening Soil model, the Soft Soil parameters (Table 6) were only declared for the fine soil layers. The initial void ratio was determined from the results of mechanical tests of unaltered samples. The preconsolidation pressure (P_c'), overconsolidation ratio (OCR), compression (C_c) and reloading (C_r) indices were obtained from the results of one-dimensional consolidation tests with loading and unloading stages, in some cases correlation values with water content for clay soils in the Valley of Mexico generated by GEIC-CFE were used. The loading-reloading Poisson's ratio (ν_{ur}) for this model was set as a constant of 0.15 for all materials (Bentley, 2023).

Table 6. Building A & B Soft Soil Model.

GU	e_o	p_c' (kPa)	OCR	C_c	C_r	ν_{ur}
2						
5	2.29	---	---	1.651	0.531	0.15
8	8.26	77	3.3	7.525	0.537	0.15
10	5.46	91	1.8	10.972	0.489	0.15

6 SPECIAL SITE CONDITIONS

6.1 *Overconsolidation Ratio*

The results of the preconsolidation pressure from consolidation tests on fine-grained soils (Figure 7) are higher than those typically reported in materials from the Valley of Mexico (Auvinet et al, 2017). We attribute this consolidation to the overburden of sand layers from stratigraphic units 3 and 5, which are not normally found in the Lake area with thicknesses grosser than 1 m (Auvinet et al, 2017).

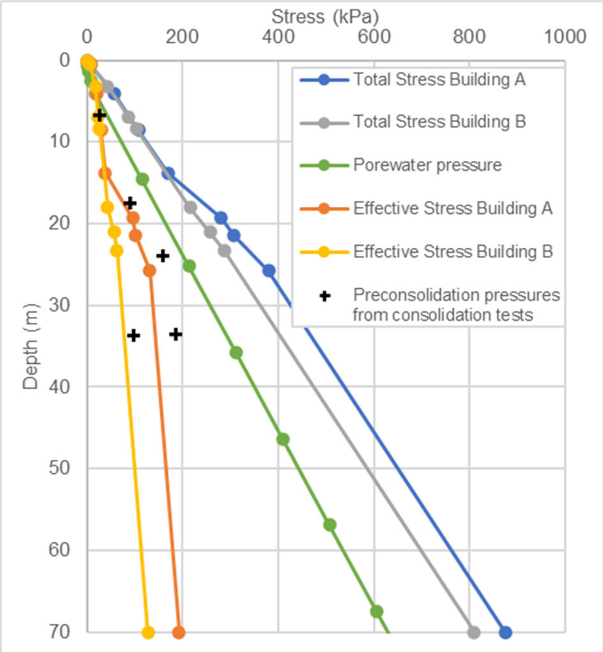

Figure 7. Vertical stress profile at the site.

6.2 *Undrained Shear Strength*

The determination of the undrained shear strength parameter is crucial in the geotechnical design of foundations because it defines the bearing capacity of shallow and deep foundations in fine-grained soils. Obtaining this parameter is a common practice using CPTu data since the correlation is relatively straightforward using the N_{kt} factor to convert corrected cone tip data to shear strength. Having data from the VST and triaxial tests allowed for the calibration of the strength parameter and N_{kt} values for this type of soil, which typically range between 12 and 13 in the literature. As a calibration exercise, Robertson's formulas (2012) were used to calibrate the N_{kt} parameter with VST results. The results for some onsite CPTu are shown in Figure 8.

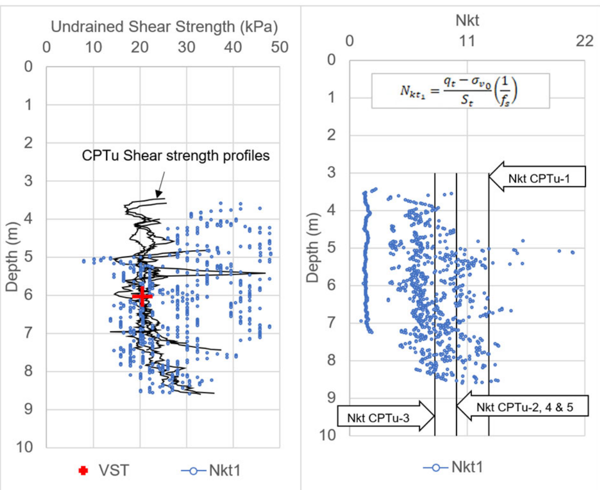

Figure 8. Undrained shear strength results and associated N_{kt} values.

6.3 *Hardening soil parameters*

When it comes to obtaining parameters for the Hardening Soil constitutive model, the load-reload triaxial and consolidation tests show that the soft clayey soil layers found on-site do not fully adhere to the relationships established in the technical literature (Bentley, 2023). One of the published relationships for this constitutive model is the correlation between the reference elastic modulus at 50% of ultimate strength and the reference oedometer modulus Equations (3a) and (3b):

$$E_{50}^{ref} = 1.25E_{oed}^{ref} \text{ for typical soils} \quad (3a)$$

$$E_{50}^{ref} = 2E_{oed}^{ref} \text{ for very soft soils} \quad (3b)$$

Regarding the correlation of the reference oedometric modulus and the modified compression index, the relationship in Equation (4) is not satisfied for these materials.

$$E_{oed}^{ref} = \frac{p^{ref}}{\lambda^*}; \lambda^* = \frac{\lambda}{(1+e_0)} \quad (4)$$

Finally, the correlations to determine the load-reload reference module (Equations (5) and (6)) based on consolidation results also do not comply with the proposed relationships.

$$E_{ur}^{ref} \approx \frac{2p^{ref}}{\kappa^*}; \kappa^* = \frac{\kappa}{(1+e_0)} \quad (5)$$

$$E_{ur}^{ref} = 3E_{50}^{ref} \quad (6)$$

Table 7 shows the comparison between the experimental results and the determinations when applying the correlations directly from Equations (3a), (3b), (4), (5), and (6) with the laboratory data. It is recommended that for these types of soft soils, the necessary tests be carried out to experimentally determine these parameters since the correlations proposed in literature may not be a representative condition.

Table 7. Parameter relationships and comparison with laboratory results.

GU	E_{50}^{ref} (kPa)	E_{ur}^{ref} (kPa)	E_{oed}^{ref} (kPa)	λ*	κ*
2	3,215		280	0.411	0.083
4	3,886	6,980	454	0.431	0.083
9	7,304	10,103	4,209	0.457	0.052
GU	E_{50}^{ref} (3a) (kPa)	E_{50}^{ref} (3b) (kPa)	E_{oed}^{ref} (4) (kPa)	E_{ur}^{ref} (5) (kPa)	E_{ur}^{ref} (6) (kPa)
2	350	560	243	2,410	9,645
4	568	908	232	2,410	11,658
9	8,418	8,418	219	3,846	21,912

The values entered in the numerical model had to be adjusted to be able to run the necessary simulations and are shown in Table 5.

6.4 *Dynamic conditions*

Regarding geophysical exploration, the seismic microzonation of the site determined that the fundamental periods of the site range from 0.2 to 0.22 Hz (T = 5.0 to 4.54 s, respectively). These values are higher than those reported in publications (Sísmica de Suelos, 2024 and Martinez et al, 2015), which place this zone with fundamental periods around 0.5 Hz (2.0 s). The average shear wave velocity of the 45 m analyzed in the cross-hole test is 98 m/s, which generates significant amplification effects in the structural analysis for seismic engineering. In the transparent site spectrum analysis, the peak ground acceleration a_0 is 0.5g, and the seismic coefficient is 1.1g in a plateau from 0.5 to 3.1 s.

No dynamic laboratory testing was performed to confirm in-situ testing values as it went beyond the scope of this study.

7 FOUNDATION AND EXCAVATION SOLUTION

The site conditions required both buildings to have a foundation solution consisting of a foundation box connected to driven piles with pre-drilled holes with a length of 22 m, supported in geotechnical unit 9. The combined calculated capacity of the piles in factored condition is 118,230 kN for Building A and 56,742 kN for Building B. Regarding serviceability conditions, it is estimated that the total settlement of 25 years of service for Building A will be 20 cm, while for Building B it will be 26 cm. Neither of the buildings reached the maximum allowable differential settlement greater of 0.001 radians, a limit established in the NTC-DE (GCDMX, 2023b).

Regarding the excavation system solution, it was decided to use a diaphragm wall system with a thickness of 0.80 m and a total length of 13 m, encompassing the footprint of both buildings for interconnection. This design fulfilled the ultimate limit state (shear failure and water pressure failure) requirements, and in the serviceability limit state, the displacements of the excavation were less than 1 cm in 3D numerical simulations.

Figure 9 shows a diagram of the foundations and excavation system of both buildings.

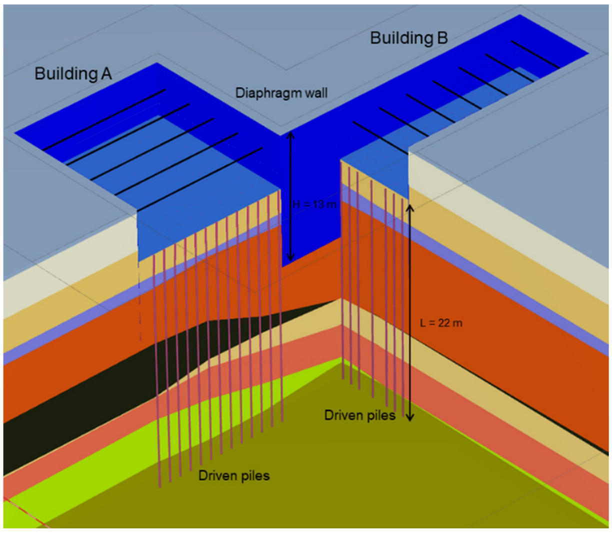

Figure 9. Mock-up of foundation solution and excavation containment system.

8 CONCLUSIONS

The explored site exhibited drastic erraticism in the condition of materials, compared to what is usually identified in the Valley of Mexico. The special site conditions required a special and expanded geotechnical exploration campaign with the addition of field tests to properly characterize the terrain. The Mexican regulations for foundation design and construction already include the tests used in this campaign for site characterization in its 2023 update (GCDMX, 2023a).

It is worth noting that the GEIC-CFE has at its disposal an extensive catalog of tools for projects to adapt to these conditions and carry out a comprehensive characterization with field tests. Additionally, it has a well-equipped laboratory to conduct strength and deformation tests under standard, cyclic, and load-unload conditions for the calibration of numerical modelling.

A key contribution of this project is the geotechnical data and instruments placed onsite that can be used as a guide for comparisons between numerical predictions and field monitoring data, which validates the design approach and provides insights into the performance of geotechnical systems in challenging seismic environments.

As attributed to Dr. Karl Terzaghi, Mexico City is considered the "paradise" of soil mechanics (Juarez and Rico, 2005) due to the unique properties of its subsoil. This geotechnical exploration underscores the need for advanced characterization engineering to develop viable foundation designs and excavation retention systems.

The final foundation design for both structures was a mixed solution: Foundation slab connected with piles with a length of 22 m driven and pre-drilled. Regarding the retention system for the excavation, a diaphragm wall with a thickness of 0.8 m and an embedment length of 13 m from the natural ground level was chosen. This study offers practical guidance for similar projects and highlights the importance of integrating high quality geotechnical data into foundation design.

9 ACKNOWLEDGEMENTS

We extend our gratitude to our colleagues from the Department of Soil Mechanics for their support and collaboration in carrying out this project, their comments, and reviews of this manuscript.

10 REFERENCES

Auvinet, G. 2019. Geotechnical Engineering in Spatially Variable Soft Soils, In: *XVI Pan-American Conference on Soil Mechanics and Geotechnical Engineering*, Cancún, Mexico, pp. 6-107. https://doi.org/10.3233/ASMGE190004

Auvinet, G., Méndez, E. and Juárez, M. 2017. *El Subsuelo de la Ciudad de México* Vol. III, II UNAM. Mexico City.

Bentley. 2023. *PLAXIS Material Models Manual 2D*, Plaxis B.V, Delft, Netherlands.

Briaud, J. L. 2023. *Geotechnical Engineering: Unsaturated and Saturated Soils*, 2nd ed., Wiley and Sons, Hoboken, United States of America. https://doi.org/10.1002/9781119788720

Budhu, M. 2011. *Soil mechanics and foundations*, 3rd ed., Wiley and Sons, Hoboken, United States of America.

Comisión Federal de Electricidad (CFE). 2018. *Manual de Diseño de Obras Civiles Capitulo B. 2. 3. Pruebas de Campo para determinar propiedades de los suelos y enrocamientos*, San Bernardino, United States of America, 2018.

Das, B. M. 2006. *Principios de Ingenieria de Cimentaciones*, 5th ed., Thomson and Learning, Mexico City, Mexico, 2006.

Díaz-Rodríguez, J. A., Leroueil, S. and Alemán, J. D. 1992. *On yielding of Mexico City clay and other natural clays*. ASCE Journal of Geotechnical Engineering 117 (7): 981-995.

Gobierno de la Ciudad de México (GCDMX). 2023a. *Normas Técnicas Complementarias para Diseño y Construcción de Cimentaciones*, Gaceta Oficial de la Ciudad de México.

Gobierno de la Ciudad de México (GCDMX) 2023b. *Normas Técnicas Complementarias sobre Criterios y Acciones para el Diseño Estructural de las Edificaciones*, Gaceta Oficial de la Ciudad de México.

Ibarra-Razo, E., et al. 2018. *Some experiences using the piezocone in Mexico. Cone Penetration Testing 2018 (CPT'18)*, Delft, The Netherlands, pp. 347-350. https://doi.org/10.1201/9780429505980

Juarez, E. and Rico, A. 2005. *Mecánica de suelos Tomo I Fundamentos de la mecánica de suelos*, Limusa, Mexico City, Mexico.

Juárez, M., Román, H., Auvinet, G. and Méndez, E. 2022. Predicción del hundimiento regional en el Valle de México, In: *XXXI Reunión Nacional de Ingeniería Geotécnica*, Guadalajara, Mexico, 2022, pp. 145-153.

Martínez, J., Lermo, J, Vergara-Huerta, F. and Ramos, E. 2015. Avances en la Zonificación Sísmica de la Ciudad de México y Zona de Chalco, Edo. de Mex., Propuesta de Nuevo Mapa de Periodos Dominantes para las NTC para Diseño por Sismo del Reglamento del D. F. In: *XX Congreso Nacional de Ingeniería Sísmica*, Acapulco, Mexico.

Robertson, P K., and K. L. Cabal. 2022. *Guide to cone penetration testing for geotechnical engineering*. 7th ed., Gregg Drilling & Testing, Signal Hill, United States of America.

Sísmica de Suelos. 2024. *Sistema de Evolución del Hundimiento y Espectros de Diseño Sísmico (SEHEDIS)*, [online] Available at: https://sismica.com.mx/sehedis/, accessed: 20/February/2024.